

Assessment of phonon mode characteristics via infrared spectroscopic ellipsometry on *a*-plane GaN

V. Darakchieva^{*,1}, T. Paskova^{1,2}, P. P. Paskov¹, H. Arwin¹, M. Schubert³, B. Monemar¹, S. Figge², D. Hommel², B. A. Haskell⁴, P. T. Fini⁴, and S. Nakamura⁴

¹ Department of Physics and Measurement Technology, Linköping University, 581 83 Linköping, Sweden

² Institute Solid State Physics, University of Bremen, 28359, Bremen, Germany

³ Fakultät für Physik and Geowissenschaften, Universität Leipzig, 04103 Leipzig, Germany

⁴ Materials Department and NCIP/ERATO JST, University of California, Santa Barbara, CA

Received 16 August 2005, accepted 23 December 2006

Published online 9 June 2006

PACS 63.20.Dj, 71.70.Fk, 78.30.Fs

Generalized infrared spectroscopic ellipsometry was applied to study the vibrational properties of anisotropically strained *a*-plane GaN films with different thicknesses. We have established a correlation between the phonon mode parameters and the strain, which allows the determination of the deformation potentials and strain-free frequency of the GaN $A_1(\text{TO})$ mode. These results are compared with previous theoretical and experimental findings and discussed.

© 2006 WILEY-VCH Verlag GmbH & Co. KGaA, Weinheim

1 Introduction

Despite the tremendous efforts directed to the fabrication of bulk GaN material, high-quality and large-size GaN substrates are still lacking. Consequently, nitride based technology still vastly relies on heteroepitaxy, which results typically in the presence of strain in the films. Strain has a major effect on all fundamental material properties and has been a subject of intense investigations. Recently, the growth of nonpolar group III-nitrides has gained a lot of attention since it offers a promising approach to overcome the deleterious effects of the built-in electric fields on a variety of device-important characteristics of the material. The growth of nonpolar nitrides is often realized on off-axis-cut sapphire substrates. This inevitably leads to the presence of anisotropic strain in the films, which provides a possibility to study new effects and imposes some challenges on measurements and analyses. The optical and structural properties of GaN films under anisotropic strain: nonpolar GaN on *r*-plane sapphire and polar GaN on *a*-plane sapphire, have been widely studied [1–5]. On the contrary, the reports on the vibrational properties of anisotropically strained GaN films are scarce. In this work we present a study of phonon modes of *a*-plane GaN films in correlation with the anisotropic strain in the films. The nonpolar material allows assessment by generalized infrared spectroscopic ellipsometry (GIRSE) of phonons with polarization parallel and perpendicular to the optical *c*-axis. For our study we chose five samples with film thicknesses between 1.14 μm and 67 μm grown on *r*-plane sapphire by metalorganic vapor phase epitaxy and hydride vapor phase epitaxy. The vibrational properties were studied by employing GIRSE at multiple angle of incidence and different sample geometries. High-resolution X-ray diffraction (HRXRD) in different measurement geometries was used to determine the in-plane and out-of plane strains in the films.

* Corresponding author: e-mail: vanya@ifm.liu.se, Phone: +46 87369987, Fax: +00 46 13142337

2 Anisotropic strain in *a*-plane GaN on *r*-plane sapphire

A schematic drawing of the relative orientations of the (11 $\bar{2}$ 0) *a*-plane GaN on (1 $\bar{1}$ 02) *r*-plane sapphire presenting the epitaxial relationships between film and substrate is shown in Fig. 1(a). It can be seen that the growth plane (*a*-plane) of the nonpolar GaN film will be under anisotropic strain because of the different lattice mismatches as well as the different thermal expansion mismatches between GaN and sapphire along the GaN [0001] and [1100] directions. Similarly, the basal hexagonal plane (*c*-plane) of the GaN film will be also anisotropically strained.

In linear elasticity theory the relation between the stress and strain tensor σ_{ij} and ε_{ij} is given by

$$\begin{pmatrix} \sigma_{xx} \\ \sigma_{yy} \\ \sigma_{zz} \\ \sigma_{yz} \\ \sigma_{xz} \\ \sigma_{xy} \end{pmatrix} = \begin{pmatrix} C_{11} & C_{12} & C_{13} & 0 & 0 & 0 \\ C_{12} & C_{11} & C_{13} & 0 & 0 & 0 \\ C_{13} & C_{13} & C_{33} & 0 & 0 & 0 \\ 0 & 0 & 0 & C_{44} & 0 & 0 \\ 0 & 0 & 0 & 0 & C_{44} & 0 \\ 0 & 0 & 0 & 0 & 0 & 2(C_{11} - C_{12}) \end{pmatrix} \times \begin{pmatrix} \varepsilon_{xx} \\ \varepsilon_{yy} \\ \varepsilon_{zz} \\ 2\varepsilon_{yz} \\ 2\varepsilon_{xz} \\ 2\varepsilon_{xy} \end{pmatrix}, \quad (1)$$

where C_{ij} are the elastic stiffness constants and the *x*-, *y*- and *z*-axes are chosen along the GaN [11 $\bar{2}$ 0], [1 $\bar{1}$ 00], and [0001] directions, respectively (see Fig. 1). Since these directions are parallel to the principal axes, the shear stress and strain components ($i \neq j$) are zero. Therefore, the knowledge of the normal strain components ($i = j$) is sufficient to fully describe the complex strain state in the *a*-plane GaN films. In order to assess ε_{xx} , ε_{yy} and ε_{zz} strain components we employed HRXRD in several measurement geometries. We measured at two azimuths the GaN 1120 and 2240 peaks in symmetric geometry, 1 $\bar{1}$ 00 and 2200 peaks in edge geometry, as well as the 0002, 0004 and 006 peaks in edge symmetric geometry. Details about the measurements and strain determination can be found in Ref. [6]. We found that the growth *a*-plane of all films is compressively strained both along the GaN [0001] and [1100] directions and the strain along the [1120] direction is tensile. The distortion of the GaN hexagon under this anisotropic strain is schematically given in Fig. 1(b). The stress component along the growth direction σ_{xx} vanishes because the surface is free to expand or contract. It follows from Eq. (1) that

$$\varepsilon_{yy} = -\frac{C_{11}}{C_{12}} \varepsilon_{xx} - \frac{C_{13}}{C_{12}} \varepsilon_{zz}. \quad (2)$$

A comparison between the experimentally determined and estimated via Eq. (2) values of ε_{yy} shows a fairly good agreement. We note however that generally the edge geometry used for the experimental

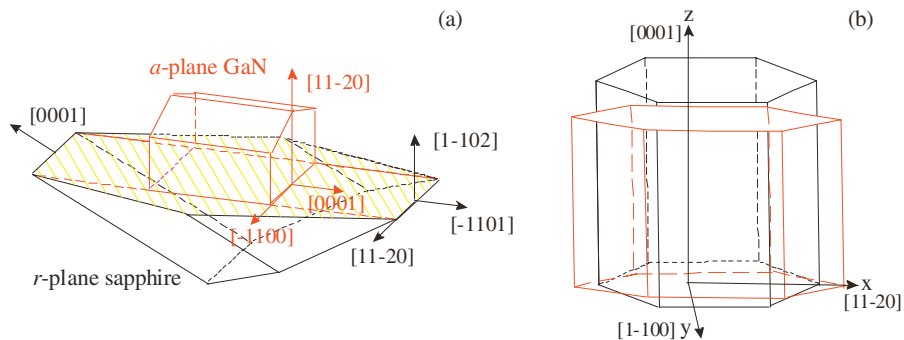


Fig. 1 (online colour at: www.pss-b.com) Schematic drawing of: (a) the relative orientations of the crystallographic axes of *a*-plane GaN on *r*-plane sapphire; (b) the distortion of the GaN unit cell under anisotropic strain.

determination of ε_{yy} and ε_{zz} leads to larger uncertainties (in particular for ε_{yy}) compared to the symmetric geometry used for the determination of ε_{xx} . Consequently, the experimentally and theoretically estimated ε_{yy} values may deviate up to 20% for some of the samples.

3 Assessment of phonon mode characteristics. GaN $A_1(\text{TO})$ deformation potentials

We used GIRSE measurements in the spectral range of 400–1550 cm^{-1} with a spectral resolution of 2 cm^{-1} in order to study the vibrational properties of the *a*-plane GaN films. The measurements were performed at azimuthal angles φ between the plane of incidence and the optical *c*-axis of the films of 0° and 90° and at two angles of incidence (60° and 70°). Because of the *a*-plane orientation of the GaN films and *r*-plane orientation of the sapphire substrates, parts of the incident p- (s-) polarized light are converted into s- (p-) polarized light which requires the application of the generalized ellipsometric approach (GE) i.e. the determination of six GE parameters: Ψ_{pp} , Ψ_{ps} , Ψ_{sp} , Δ_{pp} , Δ_{ps} and Δ_{sp} . Details about the GIRSE approach used here can be found in Refs. [7, 8]. The p–s polarization coupling, sensed by the off-diagonal elements, is small at $\varphi = 0^\circ$ and minimal at $\varphi = 90^\circ$. The sapphire substrate causes most of the p–s polarization coupling since its optical *c*-axis is tilted by $\sim 56^\circ$ with respect to the plane of incidence for the *r*-plane orientation. On the other hand most of the *a*-plane GaN films studied are thick ($\geq 15 \mu\text{m}$) and the signal from the substrate is negligible (they were modeled as free-standing in the calculation of their GIRSE spectra). Consequently, the Ψ_{ps} , Ψ_{sp} , Δ_{ps} and Δ_{sp} are noisy and particularly those at $\varphi = 90^\circ$ are even hardly measurable. The experimental and calculated diagonal GIRSE spectra are shown in Fig. 2 for one representative sample showing typical behavior. The off-axis oriented material allows access to the complete set of A_1 - and E_1 -symmetry longitudinal and transverse phonon mode and free-carrier parameters. In particular, the *a*-plane GaN offers a possibility to assess the characteristics of the $A_1(\text{TO})$ phonon mode which is not accessible via IRSE on *c*-plane oriented films. It is seen from Fig. 2 that the low-frequency edge of the GaN reststrahlen band in Ψ_{pp} and Δ_{pp} moves from $A_1(\text{TO})$ to $E_1(\text{TO})$ as the azimuth changes from 90° to 0°, because the incident electric field parallel to the film interface senses lattice excitations with polarization parallel and perpendicular to the GaN *c*-axis, respectively.

We extracted from the best-fit to the GIRSE data the frequency and broadening parameters of the TO and LO phonons with A_1 - and E_1 -symmetry, as well as the free-carrier concentrations for all samples studied. We will focus on the GaN $A_1(\text{TO})$ deformation potentials since so far only very few Raman and theo-

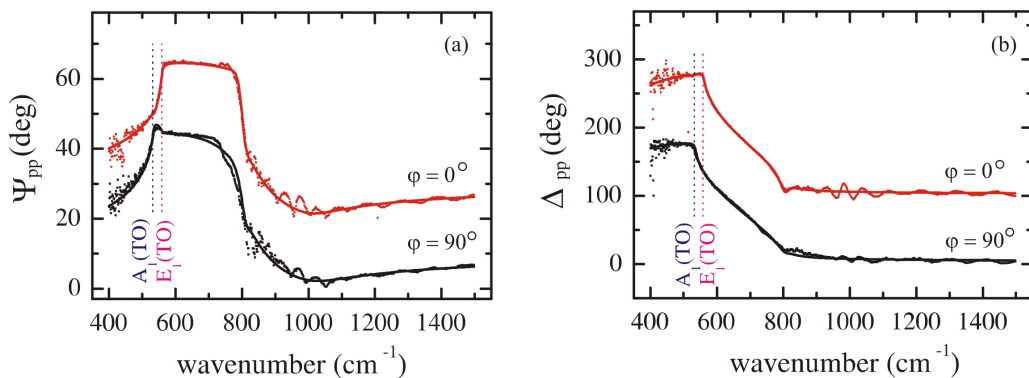


Fig. 2 (online colour at: www.pss-b.com) Experimental (dots – $\varphi = 0^\circ$; squares – $\varphi = 90^\circ$) and best-fit model calculations (solid lines – $\varphi = 0^\circ$; dashed lines – $\varphi = 90^\circ$) of GIRSE data Ψ_{pp} (a) and Δ_{pp} (b) for one representative *a*-plane GaN film with a thickness of 17 μm . Spectra for two different azimuths φ , shifted by 50° and 100° in Ψ and Δ , respectively are shown. The GaN $A_1(\text{TO})$ and $E_1(\text{TO})$ frequency positions are indicated by vertical dotted lines.

Table 1 $A_1(\text{TO})$ strain-free frequency, ω_0 , and deformation potentials, $a_{A_1(\text{TO})}$ and $b_{A_1(\text{TO})}$.

references	ω_0 (cm^{-1})	$a_{A_1(\text{TO})}$ (cm^{-1})	$b_{A_1(\text{TO})}$ (cm^{-1})
this work	531.3	-941	-1197
Raman exp. [9]	531.8	-630	-1290
theory [10]	540	-640	-695

retical studies are reported [9, 10]. Moreover, there is a discrepancy between the theoretical results and those determined by Raman and further clarification by independent experimental technique is desirable.

The shift of the $A_1(\text{TO})$ phonon of wurtzite GaN under anisotropic strain is given by [11]

$$\Delta\omega_{A_1(\text{TO})} = a_{A_1(\text{TO})} (\varepsilon_{xx} + \varepsilon_{yy}) + b_{A_1(\text{TO})} \varepsilon_{zz}, \quad (3)$$

where $a_{A_1(\text{TO})}$ and $b_{A_1(\text{TO})}$ are the $A_1(\text{TO})$ phonon deformation potentials. A regression analysis of the experimental frequencies and strains is necessary to obtain the deformation potentials. However, Eq. (3) can not be directly used as the three strain components are not independent. Using Eq. (2) the relation between the shift of the $A_1(\text{TO})$ phonon frequency and the strains can be rewritten as

$$\Delta\omega_{A_1(\text{TO})} = a_{A_1(\text{TO})} \left(1 - \frac{C_{11}}{C_{12}} \right) \varepsilon_{xx} - \left(a_{A_1(\text{TO})} \frac{C_{13}}{C_{12}} - b_{A_1(\text{TO})} \right) \varepsilon_{zz}. \quad (4)$$

Then using our experimental results about the $A_1(\text{TO})$ frequencies, ε_{xx} , ε_{zz} and the stiffness constants reported in Ref. [12] we performed a regression analysis of Eq. (4) in order to obtain the $A_1(\text{TO})$ phonon deformation potentials and strain-free frequency. The obtained values are listed in Table 1 and compared with previous theoretical and experimental results. It is seen that there is a very good agreement between the strain-free frequency values obtained by GIRSE and Raman, while the theoretical value slightly deviates. The deformation potentials we determined are both larger than the theoretical values. We note that a similar discrepancy between theory and experiment was found to be a general tendency for other phonon modes of GaN and AlN as well [10]. Our result for the $b_{A_1(\text{TO})}$ deformation potential agrees very well with the value reported in Ref. [9] while the $a_{A_1(\text{TO})}$ is larger. It is worth mentioning that the two deformation potentials are expected to have similar values for the GaN $A_1(\text{TO})$ phonon mode [10] in accordance with our findings.

In summary, we have studied the vibrational properties of a -plane GaN films with different thicknesses in correlation with the anisotropic strain in the films, which allows an assessment of the $A_1(\text{TO})$ phonon mode characteristics. We determined the GaN $A_1(\text{TO})$ phonon deformation potentials to be $a_{A_1(\text{TO})} = -941 \text{ cm}^{-1}$ and $b_{A_1(\text{TO})} = -1197 \text{ cm}^{-1}$, and the strain-free $A_1(\text{TO})$ frequency is 531.3 cm^{-1} .

Acknowledgements We are grateful to Dr. A. Kasic for fruitful discussions. V. Darakchieva would like to acknowledge support from the Swedish Research Council (VR) under contract 2005-5054.

References

- [1] M. D. Craven, P. Waltereit, F. Wu, J. S. Speck, and S. P. DenBaars, *Jpn. J. Appl. Phys.* **42**, L235 (2003).
- [2] T. Paskova, V. Darakchieva, P. P. Paskov, J. Birch, E. Valcheva, P. O. A. Persson, B. Arnaudov, S. Tungasmita, and B. Monemar, *phys. stat. sol. (c)* **2**, 2027 (2005).
- [3] V. Darakchieva, P. P. Paskov, T. Paskova, E. Valcheva, B. Monemar, and M. Heuken, *Appl. Phys. Lett.* **82**, 703 (2003).
- [4] P. P. Paskov, V. Darakchieva, T. Paskova, P. O. Holtz, and B. Monemar, *phys. stat. sol. (b)* **234**, 892 (2002).
- [5] A. Alemu, B. Gil, M. Julier, and S. Nakamura, *Phys. Rev. B* **57**, 3761 (1998).
- [6] T. Paskova, V. Darakchieva, P. P. Paskov, J. Birch, E. Valcheva, P. O. A. Persson, B. Arnaudov, S. Tungasmita, and B. Monemar, *J. Cryst. Growth* **281**, 55 (2005).

- [7] M. Schubert, in: Theory and Application of Generalized Ellipsometry, Handbook of Ellipsometry, edited by G. E. Irene and H. G. Tompkins (William Andrew Publ., Noyes Publications, Norwich, 2004).
- [8] V. Darakchieva, J. Birch, M. Schubert, T. Paskova, S. Tungasmita, G. Wagner, A. Kasic, and B. Monemar, Phys. Rev. B **70**, 045411 (2004).
- [9] V. Yu. Davydov, N. S. Averkiev, I. N. Goncharuk, D. K. Nelson, I. P. Nikitina, A. S. Polovnikov, A. N. Smirnov, and M. A. Jacobson, J. Appl. Phys. **82**, 5097 (1997).
- [10] J.-M. Wagner and F. Bechstedt, Phys. Rev. B **66**, 115202 (2002).
- [11] R. J. Briggs and A. K. Ramdas, Phys. Rev. B **13**, 5518 (1976).
- [12] M. Yamaguchi, T. Yagi, T. Azuhata, T. Sota, K. Suzuki, S. Chichibu, and S. Nakamura, J. Phys.: Condens. Matter **9**, 241 (1997).